ELSEVIER

Journal of Photochemistry and Photobiology A: Chemistry 101 (1996) 171–181

Journal of PHOTOCHEMISTRY AND PHOTOBIOLOGY A:CHEMISTRY

The photophysics of β-homo-tyrosine and its simple derivatives

Wiesław Wiczk *, Leszek Łankiewicz, Cezary Czaplewski, Stanisław Ołdziej, Krystyna Stachowiak, Alicja Michniewicz, Adam Liwo

Faculty of Chemistry, University of Gdańsk, Sobieskiego 18, 80-952 Gdańsk, Poland

Received 8 March 1996; accepted 28 May 1996

Abstract

The synthetic derivatives of β-homo-tyrosine (βHty), an analogue of tyrosine with an extra $-CH_2-$ incorporated between the carboxylic group and the CH carbon, modified at the amino group (free or acetylated), carboxyl group (free or amidated) and/or phenolic oxygen (free or methylated), were the subject of fluorescence studies and theoretical calculations in order to establish whether the rotamer model can be used to explain the fluorescence quenching of tyrosine. The *N*-acetylated derivatives of βHty with ionized carboxylate display biexponential fluorescence decay, whereas the other compounds show monoexponential fluorescence decay. Biexponential decay is assumed to be a result of the presence of low-energy conformers with a sufficiently high energy barrier to make them stable within the fluorescence timescale. The presence of stable conformers has been demonstrated by molecular mechanics and dynamics calculations. Moreover, in the case of βHty derivatives, the fluorescence quenching ability of the amide group depends on the distance between the chromophore, protonated amino and amide groups.

Keywords: β-Homo-tyrosine; Photophysics

1. Introduction

The fluorescence of tyrosine, tyrosine derivatives and tyrosine residues in peptides and proteins has been the subject of extensive investigations. The tyrosine zwitterion and derivatives with an ionized α-carboxyl group exhibit monoexponential decay kinetics. The conversion of the α-carboxyl group to the corresponding amide or its protonation results in a complex fluorescence decay [1–4]. Several explanations for the complex fluorescence kinetics of tryptophan and tyrosine have been proposed, including the involvement of ^1L_a and ^1L_b states [5–7], excited state reaction [8–10] and different lifetimes for the side-chain rotamers about the C^α–C^β bond [3,11–22]. In the rotamer model, multiexponential decay kinetics are proposed to be a result of the presence of a number of ground state rotamers, some of which do not interconvert within the fluorescence timescale (typically 3–5 ns). Individual rotamers are assumed to exhibit monoexponential decay kinetics. This model, introduced by Gauduchon and Wahl [3], suggests a charge transfer quenching between the excited aromatic chromophore (indole or phenol ring respectively) as donor and electrophilic units in the amino acid backbone (carbonyl or protonated amino group [15–17,20,21]) as acceptor. The experimental basis of the rotamer theory was the observation by Cowgill [23] that the peptide carbonyl or the amide group is responsible for the quenching of tyrosine fluorescence in proteins, and that of Tournon et al. [24] that the carbonyl groups can quench the fluorescence of aromatic rings efficiently by a charge transfer mechanism. Different rotamers will have different distances between the phenolic ring and the quenching groups (amide and/or carboxyl), which explains the differences in the photophysical behaviour of different rotamers. As shown by Laws and coworkers [1,21], the shorter fluorescence decay lifetime is associated with the protonated carboxyl group, whereas the longer lifetime is associated with ionized carboxylate. Using global and linked-function analysis, Laws and coworkers showed that the rotamer model could explain the complex fluorescence decay of tyrosine analogues [1,20] and tyrosine [20,21] and tryptophan [17] residues in small peptides. The rotamer model for tyrosine analogues and peptides containing tyrosine or tryptophan residues shows that the rotamer in which the phenol or indole ring comes into closest contact with the carbonyl group has the shortest fluorescence lifetime. From these results, it appears that the rotamer interconversion about the C^α–C^β bond in tyrosine is slower than the lifetime of the excited state. For those tyrosine components exhibiting a single-exponential decay, Laws and

* Corresponding author. Tel.: +48 58 41 52 71; fax: +48 58 41 03 57.

PII S1010-6030(96)04409-7

coworkers [1,4] were unable to establish whether the slow-exchange rotamer model was the accurate description, with the three rotamers having similar unresolved fluorescence lifetimes, or whether rotamer interconversion was fast, averaging the emission. A rotamer model has also been used to explain acrylamide quenching of tyrosine amide [22]. The charge transfer quenching between the electrophilic unit in the amino acid backbone and the excited aromatic phenol subunit leads to a biexponential fluorescence decay of tyrosine in acidic aqueous solution. This phenomenon was investigated by Kungl [25]. On the basis of the dynamics of tyrosine and the peptide Gly-Tyr-Gly in vacuo and water, with classical molecular dynamics and stochastic computer simulations, he concluded that, since the rotamers frequently interconvert within the fluorescence lifetime of tyrosine, their contribution to the non-exponential fluorescence decay should be negligible.

Molecular dynamics simulations of the conformational dynamics of tryptophan were performed by Gordon et al. [26]. They obtained different results depending on the model used for hydrogen representation in the simulation. The rotamer model for the tryptophan zwitterion can be supported using the CHARM intramolecular potential if hydrogen atoms are explicitly included in the model of tryptophan. They also showed that the predicted relative populations of tryptophan rotamers are not consistent with the experimental data. The rotamer model is not supported by the results obtained by James and Ware [27] for homo-tryptophan. In homo-tryptophan (an analogue of tryptophan with an additional methylene group separating the indole ring from the α-carbon), the α–β conformers play a less significant role than the β–γ and γ–δ conformers. Homo-tryptophan, with a much larger number of conformations, exhibits the same qualitative behaviour as tryptophan, but with somewhat larger quenching lifetimes.

In the case of β-homo-tyrosine (βHty), an additional –CH_2– group is inserted between the NH_2CH– and –COOH groups. Therefore, in βHty, compared with tyrosine, only the carboxylate group is separated from the phenolic ring by the additional –CH_2– group and the NH_2– group remains in the same position (Fig. 1). According to the Newman projection, in tyrosine there are three possible positions of the phenolic ring in relation to the carboxylate group [1,4] because of the rotation around the C^{α}–C^{β} bond. The insertion of one extra –CH_2– group in βHty introduces additional possibilities of rotation. In βHty, there is rotation about the C^{α}–C^{β} and C^{β}–C^{γ} bonds, increasing the number of possible rotamers which possess different distances between the phenol ring and the carboxylate group compared with tyrosine which possesses only three rotamers. Rotation about the C^{α}–C^{β} bond in βHty is very fast, because only two hydrogen atoms are attached to the α-carbon. The energy barrier to this rotation is similar to that of butane. Such fast rotation causes averaging of the interaction between the phenol group and carboxylate group within the excited state lifetime of the molecule. This should give monoexponential fluorescence decay of an amide of

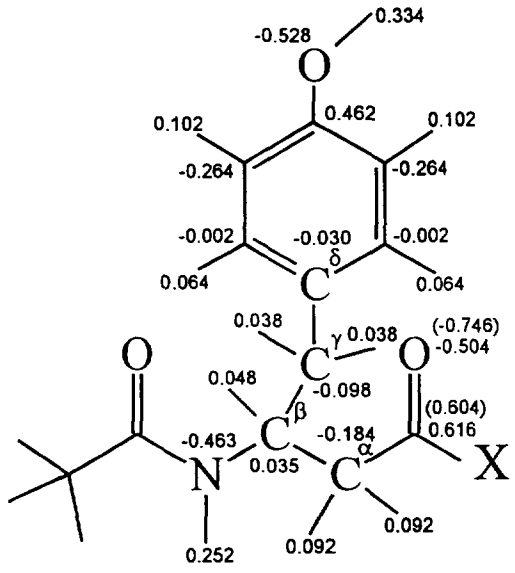

Fig. 1. Structure and partial atomic charges of βHty derivatives (X≡O$^-$ for Ac-βHty-COO$^-$ and X≡NHMe for Ac-βHty-NHMe).

βHty, which was experimentally demonstrated by Łankiewicz et al. [28] for Ac-βHty-NHMe with free and blocked hydroxyl groups. In this paper, we present the results obtained for other βHty derivatives with free and blocked amino and/or carboxyl groups in order to explain fully the influence of these groups on the photophysical behaviour of tyrosine derivatives.

2. Experimental details

2.1. Synthetic methods

The following derivatives of βHty were obtained: H-βHty-OH (βHty), H-βHty(Me)-OH (βHty(Me)), Ac-βHty-OH (Ac-βHty), Ac-βHty(Me)-OH (Ac-βHty(Me)), H-βHty-NHMe (βHty-NHMe), H-βHty(Me)-NHMe (βHty(Me)-NHMe), Ac-βHty-NHMe, Ac-βHty(Me)-NHMe. The derivatives of βHty, Boc-βHty(Bzl)-OH and Boc-βHty(Me)-OH, (Boc, tert-butyloxycarbonyl) the starting precursors for the synthesis of all the other derivatives, were obtained from the appropriate α-amino acid derivatives as described previously [29,30] in the Arndt–Eistert elongation reaction. Boc-protection removal, to prepare derivatives of βHty, was accomplished by the action of 4 N HCl–dioxane at room temperature [31].

N-Methylamides were prepared from N-Boc- and O-Me/Bzl-protected β-amino acid using PyBOP ((benzotriazolyl)-*N*-oxy-pyrrolidinium phosphonium hexafluorophosphate) as coupling reagent and H_2N-CH_3^*HCl as amine source in the presence of TEA (triethylamine) [32]. Acetylation of the amino group was realized by reaction with Ac_2O in tetrahydrofuran–H_2O. To obtain derivatives with an unprotected phenolic oxygen, the benzyl group was removed by hydrogenolysis in the presence of a catalyst (5% Pd/C). The homogeneity of the amino acid derivatives was assessed by thin

layer chromatography (TLC) (n-BuOH–AcOH–H_2O = 4 : 1 : 1, $CHCl_3$–MeOH–AcOH = 85 : 10 : 5, $CHCl_3$–MeOH = 9 : 1, AcOEt–n-hexane = 1 : 1), analytical reversed phase high performance liquid chromatography (HPLC) (a linear gradient of 0%–80% CH_3CN in 0.1% TFA (trifluoroacetic acid) in H_2O over 60 min at a flow rate of 1 ml min^{-1}; column, Kromasil C-18, 4.6 mm × 250 mm, 5 μm) and mass spectrometry (FDMS (field desorption mass spectrometry) or FABMS (fast atom bombardment mass spectrometry).

2.2. Spectroscopic measurements

Fluorescence decays were collected by the time-resolved, single-photon counting technique on an Edinburgh Analytical Instrument type CD-900 fluorometer interfaced with an IBM PC AT. The excitation source was a flash lamp filled with 0.5 atm hydrogen, operated at 40 kHz with about 6.5 kV across a 1 mm electrode gap. The half width of the instrument response was 1.2 ns. The excitation (270 nm) and emission (310 nm) wavelengths were selected by means of monochromators (about 10 nm bandwidth).

Fluorescence decays from the sample and reference (Ludox; observation wavelength, 310 nm) were measured to 4×10^4 counts in the peak. The counting rate did not exceed 2% of the lamp repetition rate. The decay curves were stored in 1024 channels of 0.054 ns per channel. The fluorescence decay data were fitted by iterative convolution to the sum of exponents

$$I(\lambda,t) = \sum_i \alpha_i(\lambda) \exp(-t/\tau_i) \quad (1)$$

where τ_i is the decay time of the ith component and $\alpha_i(\lambda)$ is its pre-exponential factor at the emission wavelength λ.

Since this model assumes that τ_i is independent of λ, the decay curves taken at different emission wavelengths can be analysed simultaneously [33,34]. The data were analysed by a global least-squares iterative convolution method supported by the manufacturer (FLA-900 Level 2 software; Edinburgh Analytical Instruments). The adequacy of the exponential decay fitting was judged by examination of plots of the weighted residuals, the statistical parameter χ^2, the shape of the autocorrelation function of the weighted residuals and the serial variance ratio (SVR). Lifetime distributions were obtained using FLA-900 Level 2 software which does not assume any functional shape of the calculated lifetime distribution.

Decay-associated spectra (DAS), the emission spectra associated with each individual decay component [35,36], were calculated from

$$I_i(\lambda) = I_{ss}(\lambda)\left[\alpha_i(\lambda)\tau_i \Big/ \sum_i \alpha_i(\lambda)\tau_i\right] \quad (2)$$

where $I_i(\lambda)$ is the emission spectrum associated with the ith component, I_{ss} is the total steady state spectrum and $\alpha_i(\lambda)\tau_i / \sum_i \alpha_i(\lambda)\tau_i$ is the fractional intensity of the fluorescence of the ith component at wavelength λ.

The steady state spectra were obtained on a Perkin–Elmer LS-50B spectrofluorometer with a 2.5 nm bandwidth for excitation and emission. The excitation wavelength was 270 nm. The quantum yields were measured relative to a value of 0.14 for tyrosine in water at room temperature [37]. In steady state measurements, the sample concentration was about 5×10^{-5} M and 1×10^{-4} M in time-resolved experiments. All measurements were performed in double deionized water (pH 7.0) at room temperature.

2.3. Molecular mechanics and molecular dynamics

The molecular dynamics (MD) simulations of βHty derivatives were carried out using the AMBER 4.0 force field [38] with the standard parameter set for amino acids [39]. Partial atomic charges were obtained by fitting to the molecular electrostatic potential (MEP) as described by Singh and Kollman [40]. The procedure was as follows. First, the geometry of βHty was optimized using the density functional theory (DFT) approach implemented in the DGAUSS program [41] with the Lee–Young–Parr functional in the 6-3G* basis set [42]. This step was necessary to obtain a reasonable geometry of βHty. Next, the MEP was calculated from the restricted Hartree–Fock (RHF) wavefunction with the 6-31G** set using the GAMESS program [43], and was subsequently employed to calculate the charges. The calculated partial charges obtained from MEP fitting are shown in Fig. 1. Initial conformations for MD simulations were generated by rotating the molecule about the C′–N–C^β–C^α, N–C^β–C^α–C, C^β–C^α–C–O and N–C^β–C^γ–C^δ dihedral angles.

Calculations were performed using the AMBER all-atom parameters on the isolated molecule without explicit solvent molecules; the solvation effect was approximated by a distance-dependent dielectric constant. Minimization was continued until the energy gradient norm decreased below 10^{-3} kcal $Å^{-1}$. Then MD simulation was performed covering a period of 100 ps. All MD simulations consisted of three steps: (1) heating from 0 to 300 K over the time period of 30 ps; (2) molecular dynamics at a constant temperature of 300 K carried out over the time period of 40 ps; (3) cooling the system from 300 to 0 K over the time period of 30 ps. A time step of 1 fs was used during all MD runs.

The energy profile was generated by maintaining the N–C^β–C^γ–C^δ dihedral angle at or close to fixed values and minimizing the energy, allowing all other variables to change freely. This method, called "adiabatic relaxation", was employed with AMBER using the CONS option in the PARM block. A harmonic constraining potential with a force constant of 400 kcal mol^{-1} was used to maintain the value of N–C^β–C^γ–C^δ within 0.5° of the desired value. The energies were computed at every point on which N–C^β–C^γ–C^δ was varied between −180° and 180° at 15° intervals.

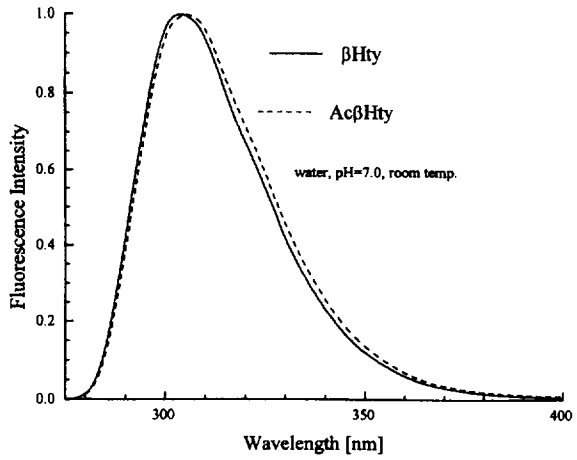

Fig. 2. Fluorescence spectra of βHty (full line) and Ac-βHty (broken line) in water at pH 7 at room temperature.

3. Results and discussion

3.1. Steady state fluorescence

The fluorescence spectra of βHty and its *N*-acetylated derivative (Ac-βHty) are shown in Fig. 2. The shapes and positions of the bands for both βHty derivatives are the same as those of tyrosine. The βHty fluorescence maximum is around 304 nm and does not shift during amidation of the carboxylate group. A small bathochromic shift (1 nm) is observed for Ac-βHty, but amidation of the carboxylate group does not influence the position of the band. Very similar effects are recorded for the *O*-methylated derivatives of βHty (with the phenolic oxygen methylated). The methylation of oxygen itself causes a blue shift of the spectral maximum by about 3 nm. The acetylation of βHty(Me) causes, as in the case of βHty, a small bathochromic shift ($\lambda_{max} = 302.5$ nm). These small but measurable shifts of the positions of the fluorescence spectral maxima are probably associated with the interaction of the amino group (protonated vs. non-protonated) with the phenolic chromophore. Also, in the case of the βHty(Me) derivative, no effect of the status of the carboxylate (free or amidated) on the band position is observed.

The fluorescence quantum yields of βHty, βHty(Me) and their monosubstituted and disubstituted derivatives are shown in Table 1. The quantum yield of βHty is slightly smaller than that of Tyr measured in the same conditions. The methylation of the phenolic oxygen in βHty increases the fluorescence quantum yield by slightly more than 20%. Changing the ionized carboxylate in βHty into a carboxyamide (*N*-methylamide), as for Tyr, causes around 13% quenching of the fluorescence. An additional incorporation of protection on the amino group (acetyl) increases the quenching to only 15.5%. Similar effects of the derivatization of the carboxylate and/or amino group are observed for βHty(Me). The incorporation of the *N*-methylamide group causes 11% quenching of the fluorescence, whereas the combination of two protections (*N*-methylamide on the carboxylate and acetylation of the amino group) increases the quenching to about 12%. The acetylation of the amino group in βHty and βHty(Me) also induces fluorescence quenching: 14% and 12% respectively. The fluorescence quenching by the acetyl group attached to the amino group in βHty derivatives is opposite to the effect of acetylation observed for Tyr derivatives: the fluorescence quenching of Ac-Tyr (ionized carboxylate) is insignificant, whereas Ac-Tyr-NH_2 acetylation increases the quantum yield and the fluorescence decay times [4].

3.2. Decay of the fluorescence intensity

The decay times of βHty and βHty(Me) derivatives are collected in Table 1 and Fig. 3. The fluorescence decay of βHty, the parent compound, in the form of a zwitterion is monoexponential, with a decay time $\tau = 3.36$ ns, i.e. practically equal to the decay time recorded for Tyr in the same conditions. For βHty(Me), monoexponential fluorescence decay is observed, with a somewhat longer decay time ($\tau = 4.77$ ns). The decay time of βHty(Me) is slightly shorter than the decay time recorded for the respective tyrosine deriv-

Table 1
Quantum yields and fluorescence lifetimes for βHty derivatives

Compound	Quantum yield	Lifetime (ns)		Pre-exponential factor		χ^2_R	
		τ_1	τ_2	α_1	α_2	1 exp	2 exp
Tyr	0.140	3.35	–	1.000	–	0.98	–
βHty	0.135	3.36	–	1.000	–	0.93	–
βHty(Me)	0.164	4.77	–	1.000	–	0.95	–
Ac-βHty	0.098	2.77	–	1.000	–	2.27	–
		1.85	3.25	0.506	0.494	–	0.98
Ac-βHty(Me)	0.134	3.76	–	1.000	–	3.38	–
		2.38	4.39	0.499	0.501	–	0.86
Ac-βHty(Me)-NHMe	0.137	4.06	–	1.000	–	0.99	–
Ac-βHty-NHMe	0.114	2.89	–	1.000	–	1.07	–
βHty(Me)-NHMe	0.138	4.11	–	1.000	–	1.04	–
βHty-NHMe	0.118	3.02	–	1.000	–	1.08	–

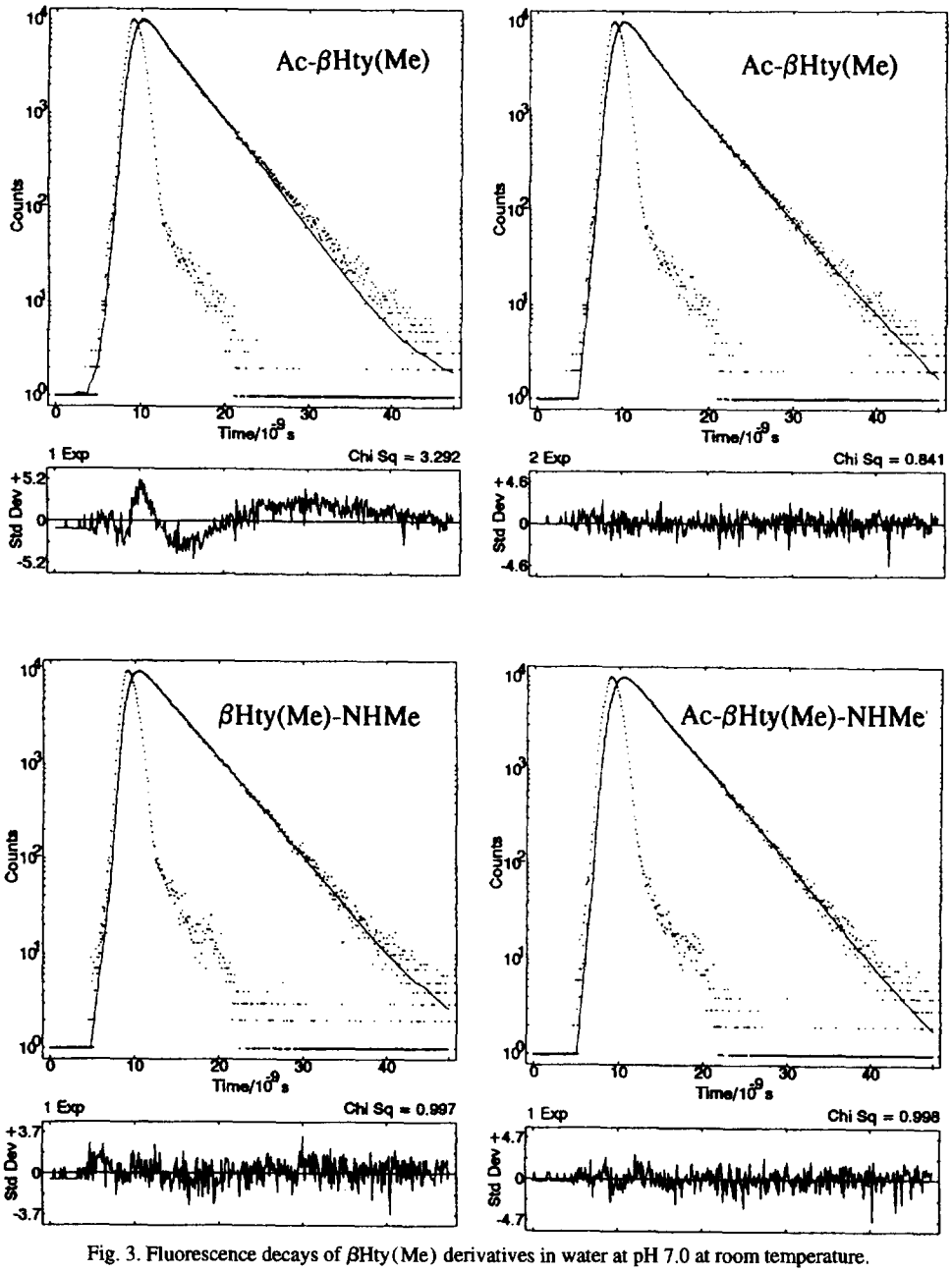

Fig. 3. Fluorescence decays of βHty(Me) derivatives in water at pH 7.0 at room temperature.

ative (Tyr(Me)) (τ=5.06 ns) [1]. Monoexponential functions are also sufficient to describe well the decay of the fluorescence of βHty-NHMe and βHty(Me)-NHMe. This can be compared with the biexponential fluorescence decay discovered for Tyr-NH_2 [1,3]. A conversion of the carboxylate in βHty and βHty(Me) into *N*-methylamide results in a decrease in the fluorescence decay time by about 10%. The decay times are 3.02 ns for βHty-NHMe and 4.11 ns for βHty(Me)-NHMe. The efficiency of fluorescence quenching of the βHty derivatives by the incorporation of a methylamide moiety is significantly lower than the effect observed after the amidation of tyrosine. A literature survey of the decay time data of tyrosine amide (Tyr-NH_2) reveals that the intensity averaged lifetimes calculated from the equation

$$\langle\tau\rangle_I=\frac{\sum_i \alpha_i\tau_i^2}{\sum_i \alpha_i\tau_i} \quad (3)$$

are 1.75 ns [1] or 1.11 ns [3] (depending on the data used in the calculations), i.e. almost three times shorter than that of parent tyrosine. Despite the fact that the *N*-methylamide group in βHty is further from the chromophore than the amide group in Tyr-NH_2, the lower efficiency of fluorescence

quenching in βHty can be partially explained as a result of a difference in the acceptor characteristics of –CO–NH_2 and –CO–$NHCH_3$ groups. The donor properties of the substituents at the nitrogen of the carboxyamide group can influence the acceptor ability of the carbonyl group due to modification of the charge distribution on oxygen and carbon. The donor properties of the nitrogen substituents for the carboxyamides discussed are in the order $H < -CH_3 < -CH_2COO^-$. The acceptor properties of the resulting amides, modified by different substituents, should influence the fluorescence quenching ability of these amides. The most efficient quencher of the fluorescence of the phenolic chromophore is the –CO–NH_2 group, followed by primary and secondary amides. Confirmation of these quenching properties of the amides was obtained from studies of the average fluorescence lifetimes for the dipeptide Tyr-Gly and Tyr-NH_2 performed by Laws et al. [1] and Gauduchon and Wahl [3]. They found that the average fluorescence lifetime of Tyr-Gly is 20% longer than that of Tyr-NH_2. The particular influence of nitrogen substituents (exhibiting different donor properties) on the acceptor properties of the carboxyamide carbonyl demonstrates that quenching of the fluorescence of the phenolic chromophore occurs via a charge transfer mechanism. The monoexponential fluorescence decays observed for βHty-NHMe and βHty(Me)-NHMe can be explained by the fact that the amide moiety in the βHty derivatives is further from the chromophore (additional –CH_2– group) than in Tyr-NH_2, which causes an extra rotational freedom associated with rotation around the C^γ–C^δ bond. This freedom increases the number of possible rotamers existing in solution, and each one has a different efficiency of fluorescence quenching. However, taking into account the low activation energy of rotamer interconversion (by rotation about a single C–C bond), a large number of rotamers having a short lifetime in comparison with the fluorescence decay time cause averaging of the measured fluorescence decay times of βHty-NHMe and βHty(Me)-NHMe. Monoexponential decays are also obtained for the diprotected derivatives (amino and carboxylate groups protected) of βHty and βHty(Me). The attachment of acetyl to the amino group with the amide moiety already present in the molecule causes only a very small decrease (in the range of experimental error, around 0.1 ns) of the fluorescence decay time. This confirms the minimal quenching ability of the acetyl group when incorporated into the amidated derivatives of βHty and βHty(Me). The very small decrease in the fluorescence decay times of Ac-βHty-NHMe and Ac-βHty(Me)-NHMe caused by acetylation and the monoexponential character of the decays are opposite to the effect of acetylation found for Ac-Tyr-NH_2. The incorporation of acetyl in the tyrosine derivative does not change the nature of the decay (the decay of Ac-Tyr-NH_2 is still biexponential). Moreover, the acetylation of Tyr-NH_2 increases the decay time significantly. An increased fluorescence decay time caused by *N*-acetylation of the amino group was observed for Tyr-NH_2 by Laws et al. [1] and Gauduchon and Wahl [3]. Fluorescence decay times for Ac-Tyr-NH_2 of $\langle\tau\rangle_I = 2.26$ ns [1] and $\langle\tau\rangle_I = 1.61$ ns [3] were obtained, i.e. significantly longer than the decay times observed for Tyr-NH_2 (1.75 ns [1] and 1.11 ns [3]).

The quenching efficiency of the ammonium group in tryptophan and tyrosine has been discussed in terms of the electrostatic effect on the quenching efficiency of the carbonyl group and has not been attributed directly to a direct quenching process [3,13,44,45]. The α-ammonium substituent quenches the tryptophan fluorescence either by a proton transfer [46] or electron transfer [47,48] mechanism. In the case of the βHty derivatives studied, in which the position of the amino group (in relation to the phenolic chromophore) is exactly the same as for Tyr, a lack of an apparent effect of the protonated amino group on the fluorescence quenching efficiency of the carboxyamide group is observed. This confirms the previously published statement [44] that the protonated amino group does not quench the fluorescence but, via its charge field, increases the quenching effectiveness of the carbonyl group (through better hydration). Because of the fact that, in βHty-NHMe, the amino group is further from the carboxyamide group (by one –CH_2– unit) than in Tyr-NH_2, the influence of this group on the fluorescence quenching properties of the amide is negligible.

The shortest fluorescence decay time is observed for Ac-βHty(Me) with ionized carboxylate. The monoexponential function does not describe well the experimental fluorescence decay data giving a high reduced sum of squares ($\chi^2_R = 2.27$ for Ac-βHty and $\chi^2_R = 3.38$ for Ac-βHty(Me)). Systematic deviations can also be observed when inspecting the plot of the residuals in the calculated and observed fluorescence intensity decays (Fig. 3). On the other hand, the fluorescence decay of these acetylated derivatives of βHty can be well defined by the superposition of two exponents ($\chi^2_R = 0.98$ for Ac-βHty and $\chi^2_R = 0.86$ for Ac-βHty(Me)). The decay times (τ) obtained are as follows: 1.85 ns and 3.25 ns for Ac-βHty and 2.38 ns and 4.39 ns for Ac-βHty(Me). These two decay times provide the same contribution to the fluorescence decay (50% each) when the pre-exponential factors are normalized to unity. The longer decay times obtained for the acetylated βHty derivatives are only slightly shorter than those obtained for parent βHty and βHty(Me) respectively. This means that these components are related to the fluorescence of non-quenched species. The shorter decay times are the result of almost 50% of the fluorescence quenching. Since the ionized carboxylate does not quench the tyrosine fluorescence [4,44], the decrease in the decay time must be associated with a quenching effect of the acetyl group. A thorough analysis of the decay times and quantum yields of the acetylated and non-acetylated derivatives of βHty-NHMe and βHty(Me)-NHMe suggests a small quenching ability of the acetyl group; however, strong quenching of the fluorescence of the Phg(OH) ((p-hydroxy)phenylglycine) derivatives by the acetyl group [49] indicates that the acetyl group can be an effective quencher when the chromophore is close to it.

Steady state and time-resolved data were combined to generate DAS, which represent the relative contributions of indi-

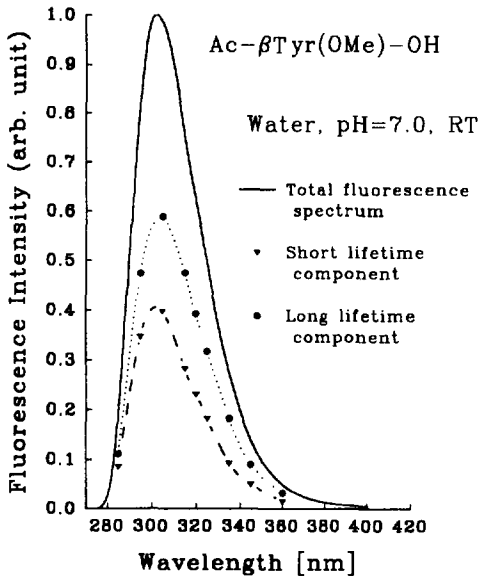

Fig. 4. Decay-associated spectra of Ac-βTyr(Me) at pH 7.0 at room temperature. The total steady state emission spectrum (full line), short lifetime component (broken line) and long lifetime component (dotted line) are shown.

vidual lifetime components, as a function of wavelength, to the total fluorescence (Fig. 4). The information from DAS can be used to assign the lifetime components to individual emitting species. The DAS for Ac-βHty(Me) excited at 270 nm shows that the 4.39 ns and 2.38 ns components have emission spectra characteristic of βHty. Since the emission of tyrosine, contrary to tryptophan, does not show any changes in the position of the fluorescence maximum with different surroundings, no conclusion can be drawn, on the basis of DAS, about the presence of two emitting species existing in different surroundings. This seems to be merely the emission of the phenolic chromophore quenched at different levels by the *N*-acetyl group.

We also performed an analysis of the distribution of the fluorescence decay times of βHty(Me) derivatives (Fig. 5). For βHty(Me), the parent compound, a narrow distribution is obtained, whereas for βHty(Me)-NHMe and Ac-βHty(Me)-NHMe, compounds with monoexponential fluorescence decays, the distributions obtained are wider. A wide decay time distribution with clearly assigned maxima is also obtained for the Ac-βHty derivatives with ionized carboxylate. This type of distribution for the derivatives with free carboxylate indicates the presence of two species, and the relatively large halfwidth of these distributions, except for the parent compounds (βHty and βHty(Me)), is a result of the presence of a large number of very similar conformers.

3.3. Conformational analysis

The minima found on the energy hypersurface of Ac-βHty and Ac-βHty-NHMe are summarized in Table 2. As shown, for Ac-βHty, the lowest energy conformation possesses an HN(Tyr)···O(COO^-) hydrogen bond closing the six-membered ring. There are two possibilities for such ring closure, differing in the orientation of the backbone $-CH_2-$ group with respect to the ring plane; corresponding conformers will hereafter be referred to as C6a and C6b. The lowest energy conformation C6a is shown in Fig. 6. For Ac-βHty-NHMe, apart from the conformations C6a and C6b, conformations with an HN(NHMe)···CO(Ac) hydrogen bond closing the eight-membered ring are also possible owing to the presence of the amide proton in the C-terminal group. These conformations, hereafter referred to as the C8-type conformers, are the lowest in energy for this compound (Table 2) and the lowest energy

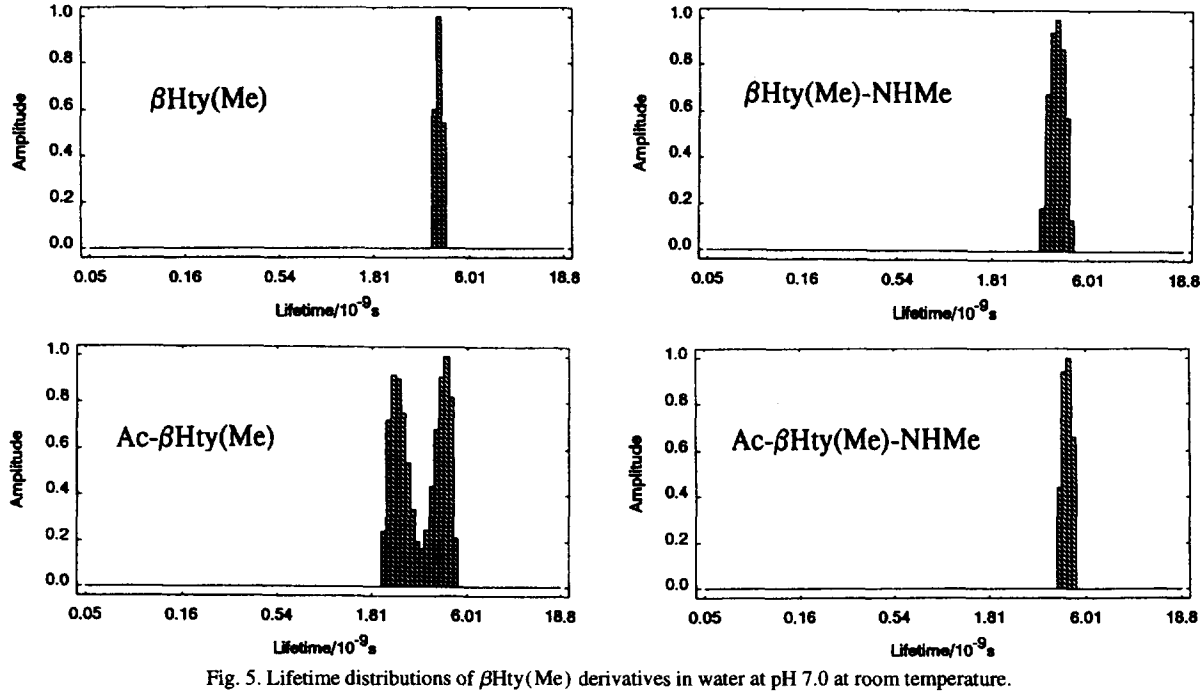

Fig. 5. Lifetime distributions of βHty(Me) derivatives in water at pH 7.0 at room temperature.

Table 2
Energies, selected dihedral angles and interchromophore distances for the low-energy conformations of Ac-βHty and Ac-βHty-NHMe

Conformer	Energy (kcal mol^{-1})	Dihedral angle				Distance	
		N–C^{β}–C^{γ}–C^{δ}	C′–N–C^{β}–C^{α}	N–C^{β}–C^{α}–C	C^{β}–C^{α}–C–N′ (C^{β}–C^{α}–C–O)	C′ON–phenyl ring centroid	CON′–phenyl ring (COO^{-}–phenyl ring) centroid
Ac-βHty							
Extended	−7.198	−167.2	−154.5	−126.0	−66.3	5.42	3.64
C6a 180[a]	−9.238	180.0	−172.0	47.5	122.8	5.51	5.75
C6a −60	−8.690	−64.6	−156.4	44.9	121.2	3.56	6.70
C6a 60	−9.746	55.5	174.7	51.3	121.3	4.36	5.75
C6b 180	−11.484	−179.2	−150.3	−56.4	−122.5	5.64	4.92
C6b −60	−11.369	−59.0	−144.4	−55.2	−132.1	3.56	6.06
C6b 60	−11.168	57.5	−153.5	−50.2	−139.1	4.68	3.69
Ac-βHty-NHMe							
Extended	−8.199	−176.9	−80.6	165.6	118.4	5.55	3.53
C6a 180	−8.628	175.4	−149.9	−61.1	−119.2	5.63	4.68
C6a −60	−8.719	−59.5	−142.8	−58.4	−124.4	3.57	6.04
C6a 60	−9.654	66.8	−152.3	−51.4	−129.5	4.88	3.45
C6b 180	−9.291	−174.9	43.4	51.9	−92.1	5.67	5.75
C6b −60	−10.020	−54.5	42.5	53.4	−91.5	4.59	6.68
C6b 60	−10.128	62.6	35.9	58.1	−92.4	3.74	5.86
C8 180[b]	−11.563	−175.6	−71.0	127.1	−65.2	5.83	4.65
C8 −60	−11.241	−58.2	−72.8	123.8	−63.8	4.75	6.39
C8 60	−10.379	56.0	−73.2	122.8	−63.6	5.14	6.07

[a]Conformations with an NH(Ac)···O(COO^{-}) hydrogen bond; a and b denote the position of the β-CH_2 group on the opposite or same side respectively of the six-membered ring closed by the hydrogen bond. The number denotes the approximate value of the N–C^{β}–C^{γ}–C^{δ} dihedral angle.
[b]Conformations with an NHMe(NH)···Ac(CO) hydrogen bond closing the eight-membered ring.

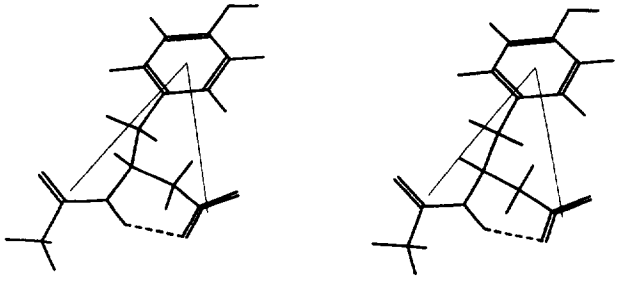

Fig. 6. Stereoview of the lowest energy conformation of Ac-βHty. The centres of the chromophore groups are linked for illustration.

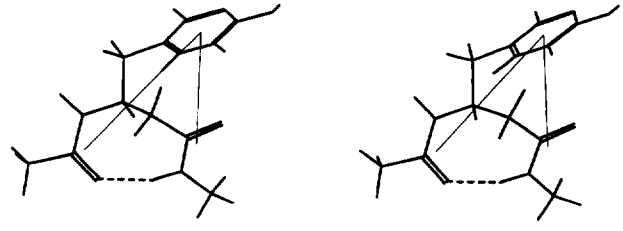

Fig. 7. Stereoview of the lowest energy conformation of Ac-βHty-NHMe. The centres of the chromophore groups are linked for illustration.

representative is shown in Fig. 7. Apart from the conformations described above, conformations with an extended backbone are also energy minima for both compounds (Table 2).

3.4. Relationship between the conformational preferences and photophysical behaviour of Ac-βHty and Ac-βHty-NHMe

As stated in Section 1, the intensity of tyrosine fluorescence quenching by the amide group(s) strongly depends on the distance between the tyrosine phenolic ring and the amide group. Therefore in order to explain the different fluorescence quenching observed in the two βHty derivatives, we carried out an analysis of the interchromophore distances obtained in conformational calculations and MD simulations.

The interchromophore distances for low-energy conformations are included in Table 2. First, it should be noted that there are two quenching groups in Ac-βHty-NHMe (namely the N- and C-terminal amide groups) and, effectively, only one in Ac-βHty (the quenching ability of the ionized carboxyl group is negligible compared with that of the amide group). From Table 2, it can be concluded that the distances between the N- and C-terminal groups and the phenolic ring are complementary for both compounds: one is long and one is comparatively short. In Ac-βHty, the lowest energy conformation has a comparatively long distance between the N-terminal group and the phenolic ring, but the second lowest energy conformation has a short distance between these two groups; therefore fluorescence quenching in these two conformers with similar energy should be different. For Ac-βHty-NHMe, because of the presence of the second (C-terminal) quenching group and the above-mentioned complementarity of distances, the shortest interchromophore distances are less differentiated than for Ac-βHty; therefore the low-energy conformations of Ac-βHty-HNMe show similar quenching ability. Therefore this compound should

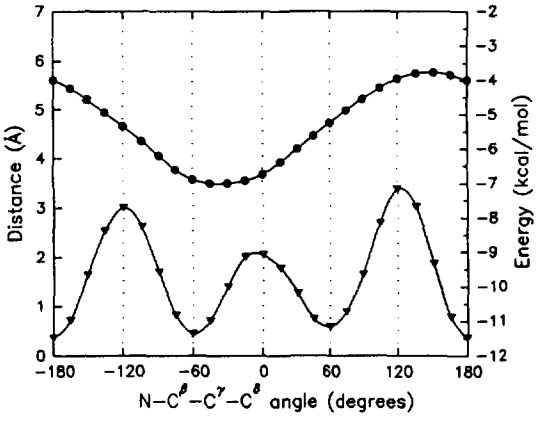

Fig. 8. Energy (triangles) and Ac...PhOH distance (filled circles) profiles for Ac-βHty-COO$^-$ corresponding to rotation about the N–C$^\beta$–C$^\gamma$–C$^\delta$ dihedral angle.

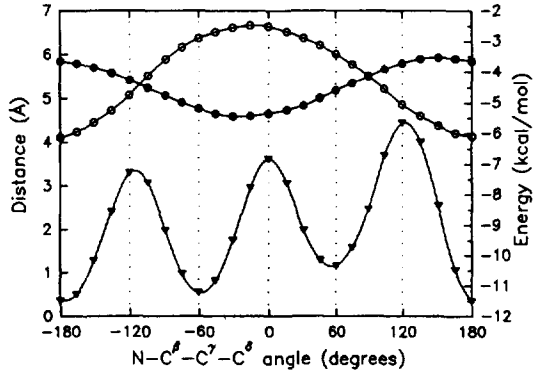

Fig. 9. Energy (triangles) and Ac...PhOH (filled circles) and PhOH...CONHMe (open circles) distance profiles for Ac-βHty-NHMe corresponding to rotation about the N–C$^\beta$–C$^\gamma$–C$^\delta$ dihedral angle.

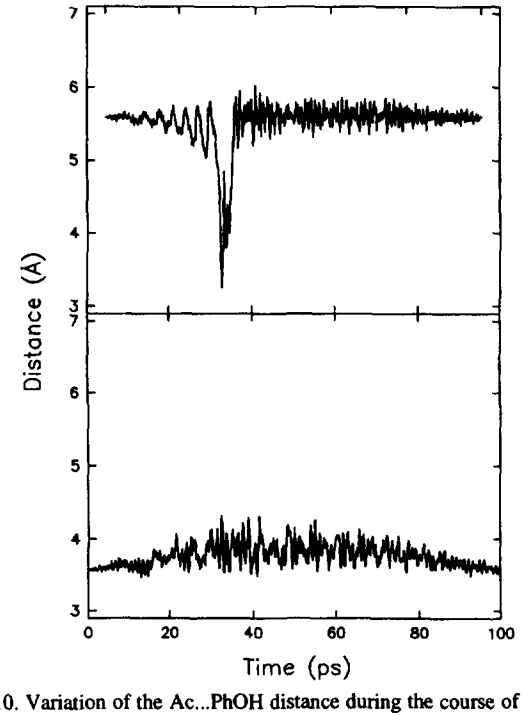

Fig. 10. Variation of the Ac...PhOH distance during the course of the MD simulation for the two lowest energy conformations of Ac-βHty-COO$^-$.

exhibit one fluorescence decay time, as observed experimentally.

In order to explain the presence of two decay times for Ac-βHty, statistical analysis is insufficient. Although different conformers should exhibit different decay times, the interconversion between them could be faster than the fluorescence timescale. In order to prove that this is not the case, we first calculated the energy and distance profiles for the rotation about the N–C$^\beta$–C$^\gamma$–C$^\delta$ angle (with which the interchromophore distance varies most significantly). For comparison, the energy and distance profiles were also calculated for Ac-βHty-NHMe. The profiles are presented in Figs. 8 and 9 for Ac-βHty and Ac-βHty-NHMe respectively. As shown, the variation in the distance as a function of the N–C$^\beta$–C$^\gamma$–C$^\delta$ angle is more pronounced for the first compound and the energy barrier between conformations is about 5 kcal mol^{-1}; this is sufficient for the conformers to be distinguished within the fluorescence timescale [18,19,50]. For the second compound, the energy barriers are also significant, but there is little variation in the shorter of the interchromophore distances as a function of the N–C$^\beta$–C$^\gamma$–C$^\delta$ angle.

The above observations are confirmed by analysing the variation in the interchromophore distance during the course of MD simulations. For Ac-βHty, when the calculations were started from conformations with different interchromophore distances, the distance only oscillated about the initial value; this suggests that it does not vary significantly within the fluorescence timescale (Fig. 10). Conversely, in the case of Ac-βHty-NHMe, the interchromophore distances converged to similar values regardless of the starting point (Fig. 11).

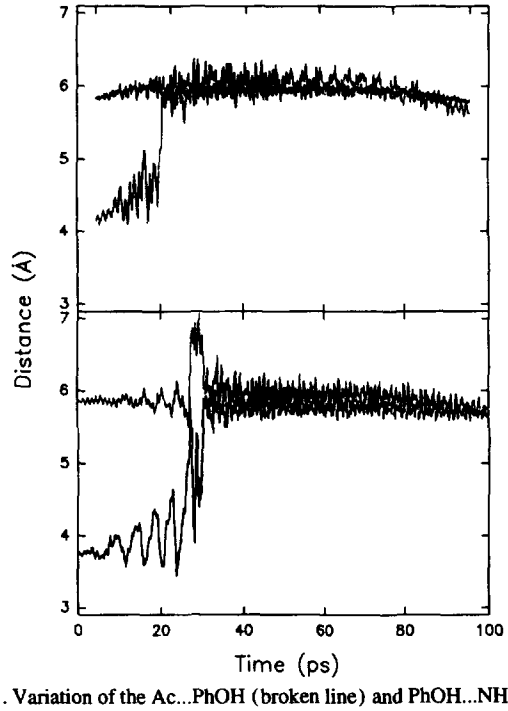

Fig. 11. Variation of the Ac...PhOH (broken line) and PhOH...NHMe (full line) distances for the two lowest energy conformations of Ac-βHty-NHMe during the course of the MD simulation.

4. Conclusions

In the rotamer model, three chemically distinct environments exist for the phenol ring, depending on the extent of rotation about the C^{α}–C^{β} bond, and each rotamer has its own associated decay constant. The relative weighting of the amplitudes is determined by the ground state rotamer populations. The existence of rotamers having different lifetimes has also been suggested as the cause of the multiexponential decay of systems containing tryptophan residues [11–16,19,45,51]. The fluorescence decay measurements for βHty derivatives have confirmed the rotamer model of quenching. MD simulations carried out for Ac-βHty-NHMe indicate that the interchromophore distance can vary almost freely within the fluorescence timescale; in contrast, for Ac-βHty, the distance only oscillates about the value characteristic of a particular low-energy conformer; this explains why the first compound has one and the second two fluorescence decay times. The results of the fluorescence decays obtained for the acetylated βHty derivatives are inconsistent with the rotamer model (the fluorescence decays are biexponential in contrast with Ac-Tyr), but they provide new suggestions regarding the quenching mechanism of the fluorescence of tyrosine analogues. The biexponential decay of the fluorescence of Ac-βHty with an ionized carboxylate group can be explained either by the formation of stable conformers, within the fluorescence timescale, with an intramolecular hydrogen bond which possesses two different distances between the phenol ring and the N-terminal group or by the coexistence of two groups of conformers with different fluorescence lifetimes. The possibility of the formation of different stable conformers makes the interpretation of the fluorescence decays of the tyrosine analogues incorporated into peptide chains rather difficult. Therefore, during the fluorescence studies of peptides or proteins containing tyrosine or its analogues, the possibility of the formation of relatively stable hydrogen bonds which can change the quenching properties of acylating groups must be taken into account.

The lack of influence of the ammonium group on the fluorescence of βHty derivatives leads to the conclusion that this group is not directly involved in the quenching process, consistent with previous suggestions [3,44]. This group influences the quenching ability of the amide group through its close proximity. The separation of the NH_3^+ group from the amide by the additional $-CH_2-$ moiety reduces considerably the quenching ability of the amide. The effect of the charge field of the NH_3^+ group and the associated better hydration of the amide group suggested by Cowgill [44] seem to provide a reasonably good explanation for the mechanism of action of the NH_3^+ group.

Acknowledgements

This work was supported by the Polish State Committee for Scientific Research (KBN) under grant PB 0582/P3/03/04.

References

[1] W.R. Laws, J.B.A. Ross, H.R. Wyssbrod, J.M. Beechem, L. Brand and J.C. Sutherland, *Biochemistry, 25* (1986) 599.
[2] J.R. Lakowicz, G. Laczko and I. Gryczyński, *Biochemistry, 26* (1987) 82.
[3] P. Gauduchon and P. Wahl, *Biophys. Chem., 8* (1987) 87.
[4] J.B.A. Ross, W.R. Laws, K.W. Rousslang and H.R. Wyssbrod, in J.R. Lakowicz (ed.), *Topics in Fluorescence Spectroscopy, Vol. 3: Biochemical Applications*, Plenum, New York, 1992, pp. 1–63.
[5] D.M. Rayner and A.G. Szabo, *Can. J. Chem., 56* (1978) 743.
[6] A.J. Ruggiero, D.C. Todd and G.R. Fleming, *J. Am. Chem. Soc., 112* (1990) 1003.
[7] J.E. Hansen, S.J. Rosental and G.R. Fleming, *J. Phys. Chem., 96* (1992) 3034.
[8] I. Saito, H. Sugiyama, A. Yamamoto, S. Muramatsu and T. Matsuura, *J. Am. Chem. Soc., 106* (1984) 4286.
[9] E. Gudgin, R. Lopez-Delgado and W.R. Ware, *J. Phys. Chem., 87* (1983) 1559.
[10] N. Vekshin, M. Vincent and J. Gallay, *Chem. Phys. Lett., 199* (1992) 459.
[11] B. Donzel, P. Gauduchon and P. Wahl, *J. Am. Chem. Soc., 96* (1974) 801.
[12] R.J. Robbins, G.R. Fleming, G.S. Beddard, G.W. Robinson, P.J. Thistlethweit and G.J. Woolf, *J. Am. Chem. Soc., 102* (1980) 6271.
[13] A.G. Szabo and D.M. Rayner, *J. Am. Chem. Soc., 102* (1980) 554.
[14] J.B.A. Ross, K.W. Rousland and L. Brand, *Biochemistry, 20* (1981) 4361.
[15] M.C. Chang, J.W. Petrich, D.B. McDonald and G.R. Fleming, *J. Am. Chem. Soc., 105* (1983) 3819.
[16] J.W. Petrich, M.C. Chang, B.D. McDonald and G.R. Fleming, *J. Am. Chem. Soc., 105* (1983) 3824.
[17] J.B.A. Ross, H.R. Wyssbrod, R.A. Porter, G. Schwartz, C.A. Michaels and W.R. Laws, *Biochemistry, 31* (1992) 1585.
[18] L. Tilstra, M.C. Sattler, W.R. Cherry and M.D. Barkley, *J. Am. Chem. Soc., 112* (1990) 9176.
[19] W.J. Colucci, L. Tilstra, M.C. Sattler, F.R. Fronczek and M.D. Barkley, *J. Am. Chem. Soc., 112* (1990) 9182.
[20] J.B.A. Ross, W.R. Laws, A. Buku, J.C. Sutherland and H.R. Wyssbrod, *Biochemistry, 25* (1986) 607.
[21] J.B.A. Ross, W.R. Laws, J.C. Sutherland, A. Buku, P.G. Panayotis, G. Schwartz and H.R. Wyssbrod, *Photochem. Photobiol., 44* (1984) 365.
[22] P.B. Contino and W.R. Laws, *J. Fluorescence, 1* (1991) 5.
[23] R.W. Cowgill, *Biochim. Biophys. Acta, 133* (1967) 6.
[24] J.E. Tournon, E. Kuntz and M.A. Bayoumi, *Photochem. Photobiol., 16* (1972) 425.
[25] A.J. Kungl, *Biophys. Chem., 45* (1992) 41.
[26] H.L. Gordon, H.C. Jarrell, A.G. Szabo and R.L. Somorjai, *J. Phys. Chem., 96* (1992) 1915.
[27] D.J. James and W.R. Ware, *Chem. Phys. Lett., 120* (1985) 450.
[28] L. Łankiewicz, J. Łanoszka, S. Ołdziej and W. Wiczk, *Amino Acids, 10* (1996) 197.
[29] L. Łankiewicz, D. Glanz, Z. Grzonka, J. Slaninova, T. Barth and F. Fahrenholz, *Bull. Pol. Acad. Sci., 37* (1998) 45.
[30] K. Plucińska and B. Liberek, *Tetrahedron, 43* (1987) 3509.
[31] G.L. Stahl, R. Walter and C.W. Smith, *J. Org. Chem., 43* (1978) 2285.
[32] J. Coste, D. Le Nguyen and B. Castro, *Tetrahedron Lett., 31* (1990) 205.
[33] J.R. Knutson, J.M. Beechem and L. Brand, *Chem. Phys. Lett., 102* (1983) 501.
[34] J.M. Beechem, E. Gratton, M. Ameloot, J.R. Knutson and L. Brand, in J.R. Lakowicz (ed.), *Topics in Fluorescence Spectroscopy, Vol. 2: Principles*, Plenum, New York, 1991, pp. 241–305.
[35] J.R. Knutson, D.G. Walbridge and L. Brand, *Biochemistry, 21* (1982) 4671.
[36] K.J. Wilis, A.G. Szabo, J. Drew, M. Zuker and J.M. Ridgeway, *Biophys. J., 57* (1990) 183.

[37] R.F. Chen, *Anal. Lett., 1* (1964) 35.
[38] D.A. Pearlman, D.A. Case, J. Caldwell, G. Seibel, U.C. Singh, P.A. Weiner and P.A. Kollman, AMBER 4.0, University of California, San Francisco, CA, 1989.
[39] S.J. Weiner, P.A. Kollman, D.A. Case, U.C. Singh, C. Ghio, G. Alagona, S. Profeta and P. Weiner, *J. Am. Chem. Soc., 106* (1984) 765.
[40] U.C. Singh and P.A. Kollman, *J. Comput. Chem., 5* (1984) 129.
[41] DGAUSS, Version 2.3, Cray Research, Engan, USA, 1992.
[42] C. Lee, W. Young and R.G. Parr, *Phys. Rev. A, 37* (1988) 785.
[43] M.W. Schmidt, K.K. Baldridge, J.A. Boatz, S.T. Elbert, M.S. Gordon, J.J. Jensen, S. Kosecki, N. Matsunaga, K.A. Nquyen, S. Su, T.L. Windus, M. Dupuis and J.A. Montgomery, *J. Comput. Chem., 14* (1993) 1347.
[44] R.W. Cowgill, in R.F. Chen and H. Edelhoch (eds.), *Biochemical Fluorescence: Concepts*, Vol. 2, Marcel Dekker, New York, Basle, 1976, Chapter 9.
[45] J. Feitelson, *Isr. J. Chem., 8* (1970) 241.
[46] S.S. Lerher, *J. Am. Chem. Soc., 92* (1970) 3459.
[47] D.V. Bent and E. Hayon, *J. Am. Chem. Soc., 97* (1975) 2612.
[48] R.F. Steiner and E.P. Kirby, *J. Phys. Chem., 73* (1969) 4130.
[49] W. Wiczk, K. Stachowiak, C. Czaplewski, L. Łankiewicz and A. Michniewicz, *J. Photochem. Photobiol. A: Chem.*, submitted for publication.
[50] H.-T. Yu, M.A. Vela, F.R. Fronczek, M.L. McLaughlin and M.D. Barkley, *J. Am. Chem. Soc., 117* (1995) 348.
[51] T.E.S. Dahms, K.J. Wilis and A.G. Szabo, *J. Am. Chem. Soc., 117* (1995) 2321.